Earth Surface Processes and Landforms
Earth Surf. Process. Landforms **24**, 1009–1024 (1999)

SPATIAL VARIABILITY OF SOILS DEVELOPING ON BASALT FLOWS IN THE POTRILLO VOLCANIC FIELD, SOUTHERN NEW MEXICO: PRELUDE TO A CHRONOSEQUENCE STUDY

M. C. EPPES* AND J. B. J. HARRISON

Department of Earth and Environmental Science, New Mexico Institute of Mining and Technology, Socorro, New Mexico 87801, USA

Received 2 April 1997; Revised 17 January 1999; Accepted 29 March 1999

ABSTRACT

If the systematic spatial variability of soils in a chronosequence is identified and accounted for, the accuracy of quantitative data derived from soil chronosequence studies will be increased. A sample design using landscape positions with minimal variability could result in more accurate chronofunctions from these studies. Four basalt flows in the Potrillo volcanic field, southern New Mexico, with ages ranging between 20 ka and 260 ka ($^{40}Ar/^{39}Ar$ and/or cosmogenic ^{3}He methods) provide a sound basis for a soil chronosequence study. Basalt flow surface relief in the Potrillos reduces with time as depressions fill with basalt rubble and aeolian dust. Soil variability is primarily a function of landscape position with respect to ridges and swales in the *original* basalt flow topography. Soils developing over original topographic lows (swale soils) form primarily in aeolian dust, have larger amounts of total carbonate and soluble salts, and display greater variability than soils developing over original topographic highs (ridge soils). It is thus concluded that ridge soils, which have minimal variability, should be employed for a soil chronosequence study of basalt surfaces in the Potrillo volcanic field.

The spatial variability of swale soils results in part from the significant hydrologic variability of low-lying landscape positions. Depth profiles of chloride concentrations suggest that hydrologic variability systematically correlates with the size and shape of depressions in which soils are forming. The infilling of depressions with aeolian material results in increasingly arid hydrologic conditions both by increasing the volume of aeolian material that is being drained and by reducing the catchment area for runoff into the depression. Depressions fill at different rates, however, depending on their size, shape and catchment area. Small, narrow depressions fill quickly, and their associated soils form under more arid conditions and have stronger development than soils in large depressions. Therefore, a number of geomorphic surfaces of varying age may develop on a single isochronous basalt flow. Each of these surfaces will have unique hydrologic characteristics and consequently different degrees of soil development. The pre-burial high water flux evident in depressions suggests that basalt flows may play an important role in aquifer recharge in this area of New Mexico.

KEY WORDS: aquifer recharge, spatial variability; chronofunction; chronosequence; arid soils

INTRODUCTION

Soils are accessible and effective tools for dating and correlating geomorphic surfaces. Rates of soil development (either qualitative or quantitative) must be described, however, before soils can be effectively employed for these purposes. Typically, regional rates of soil development are derived from a local soil chronosequence study. While qualitative estimations of soil development have been widespread (e.g. via stages of carbonate development, development indices, etc.), accurate *quantitative* determinations of soil development rates from chronosequence data have been limited owing to the large error associated with chronofunctions (functions describing soil development versus time; Switzer *et al.*, 1988; Barrett and Schaetzl, 1993; Schaetzl *et al.*, 1994). Sources of chronofunction error include: poor age control for geomorphic surfaces, inadequate sampling on each surface, and spatial variability of soils on supposedly isochronous surfaces (Bockheim, 1980; Harrison *et al.*, 1990; Harrison and Yaalon, 1992). With an ever-increasing need to accurately date geomorphic surfaces that have no age control other than soils, it is critical that chronofunction error be reduced in future chronosequence studies.

* Correspondence to: M. C. Eppes, Department of Earth and Planetary Sciences, Rm 122 Northrop Hall, University of New Mexico, Albuquerque, NM 87131, USA. E-mail: meppes@unm.edu

CCC 0197-9337/99/111009–16 $17.50

Spatial variability of soils has been recognized as a significant contributor to inaccuracy in chronofunctions. Only a handful workers, however, have attempted to account for that variability within the methodology of their soil chronosequence studies (e.g. Barrett and Schaetzl, 1993; Harrison *et al.*, 1990; Sondheim and Standish, 1983). Spatial variability in soil landscapes can be characterized as either random variability or systematic variability (Wilding and Dress, 1983). Soil variability that is classified as random is not necessarily statistically random, but rather is variability that cannot be readily attributed to geomorphic processes. Systematic variability, however, can be ascribed to known processes affecting the soil landscape. If systematic variability is identified and 'eliminated' through sampling design, then the accuracy of chronofunctions derived from a chronosequence study will improve (Harrison *et al.*, 1990).

Systematic variability is typically quantified using statistical methods. Unfortunately, in soil science it is logistically difficult to sample a large enough population on a single surface for random and systematic spatial variability to be statistically differentiated (Wilding and Drees, 1983; Sondheim and Standish, 1983; Switzer *et al.*, 1988; Harrison *et al.*, 1990). We propose that the systematic spatial variability of a soil landscape must be identified *before* temporal variability of that landscape can be addressed. Here, the authors are restating the concepts of Jenny (1941), that soil development can be described as a function of the relative contributions of climate, organisms, relief, parent material, time and other geomorphic factors [S = f (cl, o, r, p, t . . .)]. We emphasize, however, that before accurate estimations of soil development rates can be made, the relative influences of variables other than time must be minimized not only between surfaces of different ages, but also between different landscape positions on isochronous surfaces. Once those landscape positions with minimal systematic spatial variability are identified, it will be possible to minimize overall spatial variability in the chronosequence through sampling of those positions. Chronofunctions derived from soils sampled using this stratified random sample design will contain less error than those derived from a simple random population.

BACKGROUND

Basalt flows of the Potrillo volcanic field in southern New Mexico (Figure 1) provide an excellent locality for a soil chronosequence study. Recent advances in radioisotope technology have increased the accuracy and precision with which young basalt flows can be dated. Both $^{40}Ar/^{39}Ar$ and cosmogenic ^{3}He surface-exposure age dating methods give accurate dates for young basalt flow surfaces (McDougall and Harrison, 1988; Cerling, 1990; Anthony and Poths, 1992). Basalt flows of the Potrillos have been dated using both methods (E. Anthony *et al.*, unpublished data; W. McIntosh *et al.*, unpublished data). Furthermore, the Potrillo volcanic field is located in the vicinity of another soil-geomorphic/chronosequence study, the Desert Project (Gile *et al.*, 1981). Differences, if any, between the often-cited rates of soil development of the Desert Project and those of a nearby location with better age control would be of interest to many workers. Finally, previous studies of basalt flow geomorphology (Wells *et al.*, 1985; Slate *et al.*, 1991) and of spatial variability in desert regions (e.g. Yair, 1987; Yair and Shachak, 1987) provide a background for understanding the spatial variability of soils in the Potrillo volcanic field.

Basalt flow surface topography is modified dramatically with time as demonstrated by soil geomorphic studies in both the Cima and the Pinacate volcanic fields, California (Wells *et al.*, 1985; Slate *et al.*, 1991). Young basalt surfaces are extremely irregular with high relief and depressions of varying size. This morphology originates from collapse of lava tubes and from buckling of the flow surface during emplacement of the basalt flow. The resulting depressions are metres to hundreds of metres in diameter and up to 5 m deep. In arid regions, bedrock runoff can significantly increase moisture conditions at the base of such hillslopes (e.g. Yair, 1987; Yair and Shachak, 1987). Basalt flow depressions accumulate aeolian dust and basalt rubble, however, decreasing exposure of bedrock on the basalt flow surface through time (Wells *et al.*, 1985). It is possible that runoff could none-the-less provide extra moisture to the base of depressions before significant amounts of aeolian material accumulate. Wells *et al.* (1985) found that bedrock becomes covered and original basalt flow morphology is no longer evident on flows ranging in age from *c*. 250–750 ka. Processes of erosion become dominant and bedrock surfaces are re-exposed on flows older than *c*. 750 ka.

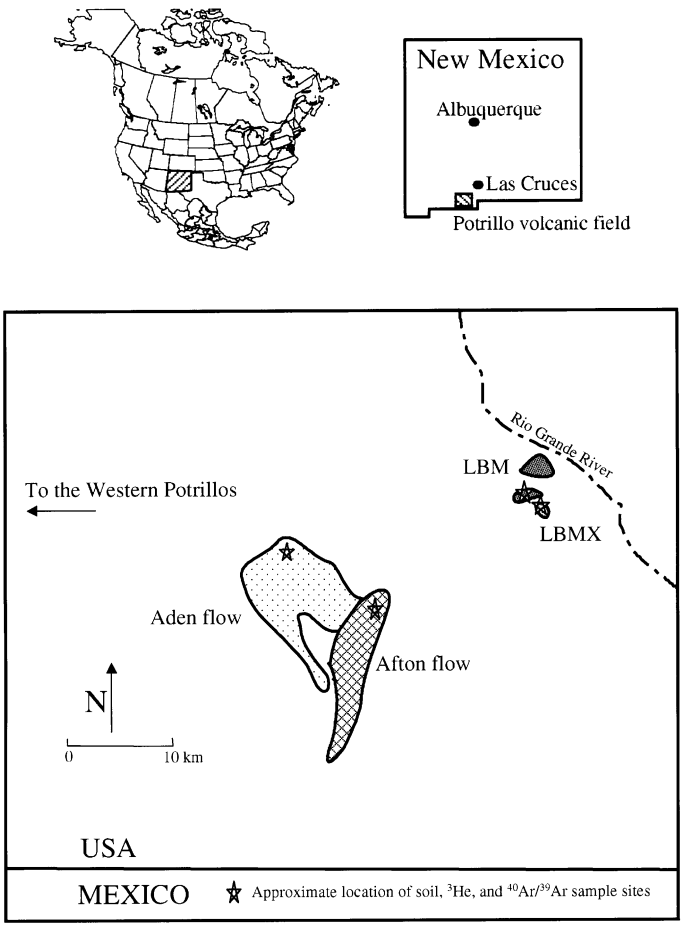

Figure 1. Location of study area, basalt flows and sample sites in the Potrillo volcanic field

We observe a similar overall evolution of topography in basalt flows of the Potrillo volcanic field. Basalt surfaces examined for this study, however, are relatively young and appear to be in various stages of aeolian mantle accumulation. We therefore expect that overall soil variability on these surfaces will be a systematic function of landscape position relative to topographic lows and highs of the original basalt flow topography. This study seeks to improve the accuracy of a future soil chronosequence study in the Potrillo volcanic field by: (1) further evaluating the evolution of basalt flow surface topography with time; (2) identifying the systematic variability of soils developing on these basalt flows; and (3) determining which landscape positions are most suitable for a chronosequence study.

THE POTRILLO VOLCANIC FIELD

Geologic setting and age control

The Potrillo volcanic field lies in the axis of the Rio Grande rift, about 40 km southwest of Las Cruces, New Mexico (Figure 1). The *c*. 1000 km^2 region is located within a major intermontane basin of the Mexico Highland section of the Basin and Range Province (Hoffer, 1976). The floor of the basin, the Upper and

Table I. $^{40}Ar/^{39}Ar$ and ^{3}He dates obtained for the AD, AF, LBM and LBMX flows in the Potrillo volcanic field

Surface	$^{40}Ar/^{39}Ar$ dates*(ka)	^{3}He dates†(ka)	Age of surface (weighted mean, ka)
AD	13 ± 11	$24 \pm 3{\cdot}5$	23 ± 3
AF	70 ± 14	103 ± 5	102 ± 4
		110 ± 7	
		94 ± 15	
LBM	188 ± 9	–	185 ± 6
	167 ± 21		
	186 ± 9		
	179 ± 17		
LBMX	263 ± 19	–	263 ± 19

* W. McIntosh *et al.*, unpublished data
† E. Anthony *et al.*, unpublished data

Lower La Mesa surfaces, are 500 ka and 700 ka respectively (Gile *et al.*, 1981). The numerous cinder cones and basalt flows of the Potrillo volcanic field were extruded onto the Upper La Mesa surface.

The basalt flows of the Potrillo volcanic field are nepheline normative, and chemically resemble other young alkaline lavas within the Basin and Range Province (Anthony and Poths, 1992). Individual flows show little geochemical variation relative to one another. The lavas are vesicular, with pahoehoe structures visible on many surfaces. The field is divided into three areas: the older Western Potrillos, a large strip of overlapping fissure-fed flows and cinder cones; the centre of the field, a broad area of two younger flow complexes (Aden and Afton); and the eastern portion of the field, an alignment of cinder cones and associated flows (Little Black Mountain flows). Four easily distinguishable flows were chosen for this study: Aden (AD), Afton (AF), and two flows from Little Black Mountain (LBM and LBMX; Figure 1).

$^{40}Ar/^{39}Ar$ and/or ^{3}He surface exposure dates have been obtained for the AD, AF, LBM and LBMX basalt flows (E. Anthony *et al.*, unpublished data; W. McIntosh *et al.*, unpublished data; Table I). $^{40}Ar/^{39}Ar$ and ^{3}He ages agree within 1σ for the AD surface and 2σ for the AF surface. Weighted means of age data are used for calculations in this study (Table I). 1σ error in the average of each surface age represents approximately 15 per cent of the age of the AD surface and *c*.5 per cent of that of the AF, LBM and LBMX surfaces.

Climate, vegetation and geomorphology

The climate of the Potrillo region is arid to semi-arid with *c*.30 cm a^{-1} precipitation (US Weather Bureau, 1996). Winds are strongest in the spring, and dust storms are common. The AD, AF, LBM and LBMX flows are vegetated with creosote, mesquite, various cacti and grasses. Relative abundances of these plants differ depending on the age of the surface and topography. In general, younger surfaces (AD and AF) have greater biodiversity than older surfaces (LBM and LBMX). There is a marked difference in vegetation between topographic highs and lows on the AD and AF flows, where highs are vegetated with different species (typically shrubs) from lows (typically grasses). Both grasses and shrubs are present throughout the LBM and LBMX surfaces, but vegetation growing over infilled depressions is larger and denser than that growing over topographic highs.

Topographic depressions on basalt flow surfaces in the Potrillo volcanic field decrease in size and number with increasing age due to the infilling of swales with basalt rubble and aeolian dust. Only small depressions (<3 m^2 surface area) on the 20 ka AD surface are completely infilled, while almost all of the original topography of the 185 ka LBM and 260 ka LBMX flows is masked by aeolian deposits. Through excavations of these older surfaces and through observations of vegetation differences, it was found that a number of large (>20 m^2, *c*.4 m deep) infilled swales are present. Depressions of similar dimensions on the AD surface remain unburied and are sometimes interconnected (Figure 2). Only swales larger than 100 m^2 remain unburied on the 100 ka AF surface.

Figure 2. Photograph of Aden (AD) basalt flow (*c*. 20 ka)

METHODOLOGY

Field and laboratory

A total of 19 soils were sampled on both ridges and swales of the four basalt flows. Ridges are defined as areas where the basalt flow surface is either: (a) a current topographic high, or (b) within 1 m of the top of the current geomorphic surface (Figure 3). Swales are defined as areas where the basalt flow surface is currently either: (a) in a topographic low relative to a ridge, or (b) deeper than 1 m below the top of the current geomorphic surface. Hereafter, soils investigated on these landscape positions will be referred to as ridge soils and swale soils.

Three ridge soils and three swale soils were described on the AD and AF surfaces, four ridge soils and one swale soil on the LBM surface, and two ridge soils on the LBMX surface. (Swale soils were not examined on the LBMX surface for logistical reasons.) All pits were located within 5 km of flow perimeters and near sites

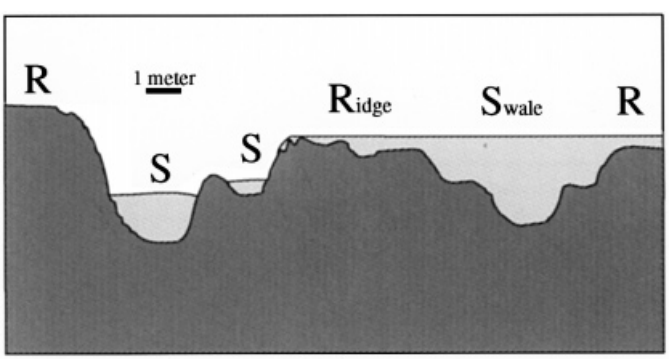

Figure 3. Schematic representation of ridge (R) and swale (S) sites on a basalt flow

where flows were sampled for dating (Figure 1). Swale pits were excavated with a backhoe with the exception of AF-S-3 (an 'S' in sample designation represents swale, and 'R', ridge), which we were unable to access with the backhoe. Ridge pits were excavated by hand or with a jackhammer. Pits on both ridges and swales were excavated until 10–40 cm of a coarse rubble zone (assumed to be the top of the original basalt flow) was exposed. This rubble zone was not reached in AF-S-3, although basalt clasts were present in the bottom 20 cm of the pit.

Soils were described and sampled using methods summarized by the Soil Survey Staff (1951,1975). In addition, average carbonate rind thickness, average clast size, and volume percentage of gravels were estimated for each horizon in all profiles. Laboratory analyses for all profiles included: bulk density, pH, soluble salts (by electrical conductivity), particle size, and percentage $CaCO_3$ of the < 2 mm portion (by Chittick method). Soil-water chloride concentrations were measured for swale soils, with the exception of AF-S-3. Standard procedures were used for all analyses (Singer and Janitzky, 1986).

Calculation of profile mass of carbonate

Soil profile mass of carbonate is usually calculated using the fine earth (<2 mm) portion of a sample (e.g. Gile *et al.*, 1981; Machette, 1985; Slate *et al.*, 1991). In coarse deposits, however, a significant amount of carbonate is found in clast coatings. Estimates of this volume of $CaCO_3$ are required to quantitatively determine the profile mass of carbonate in a soil (McDonald, 1994). Here, the horizon volume percentage of $CaCO_3$ in clast coatings was approximated using observed average clast size and average coating thickness for each horizon:

$$\text{Horizon volume \% of } \mathrm{CaCo_3} \text{ rind } (\%R) = (1 - VC/VCc)\%G$$

where VCc = volume (cm^3) of average clast size with coating, VC = volume (cm^3) of average clast size without coating, $\%G$ = volume percentage of gravels in horizon.

An average bulk density of 2·2 g cm^{-3} was assigned to the coatings. The following equation was used to calculate an approximate total mass of $CaCO_3$ in each horizon:

$$\mathrm{CaCO_3}(\text{g cm}^{-2}/\text{horizon}) = [\{BDs\%Cs(1 - \%G)\} + (\%RBDc)]HT$$

where BDs = bulk density (g cm^{-3}) of the <2 mm portion of sample, $\%Cs$ = weight percentage of $CaCO_3$ in the <2 mm portion of sample, $\%G$ = volume percentage of gravels in each horizon, $\%R$ = volume percentage of $CaCO_3$ rind in each horizon, BDc = (2·2 g cm^{-3}) average bulk density of $CaCO_3$ rinds, HT = (cm) horizon thickness.

Horizon values were then summed to obtain profile mass of carbonate for each soil profile. Similarly, a profile sum of electrical conductivity was also calculated. To aid in comparisons, the thickness of the lowest horizon in each profile was normalized to 10 cm in ridge soils and 20 cm in swale soils. It should be noted that the loss of $CaCO_3$ through the basalt fractures at the base of these soils was not accounted for by the profile mass of carbonate calculations.

RESULTS AND DISCUSSION

Systematic spatial variability between ridge and swale soils

Morphology. There are marked morphologic differences between soils developing over ridges and swales of basalt flows in the Potrillo volcanic field (Figure 4; Table II). Ridge soils typically develop in basalt fractures where aeolian material has accumulated. Development is limited to these fractures on the 20 ka AD surface. Ridge soils on older surfaces often contain a thin veneer of dust overlying a calcic horizon within the rubble zone of the underlying basalt flow. Carbonate precipitation seemingly continues into the underlying basalt via fractures to unknown depths in ridge profiles. The thickness of clast $CaCO_3$ coatings in ridge soils

Table II. Field descriptions of typical ridge and swale soils in the Potrillo volcanic field

Soil	Age (−ka)	Horizon	depth (cm)	Structure	Texture	Consistency		Colour		Gravel %; Pores	Carbonates
						Moist	Dry	Moist	Dry		
AD-R-4	19	A	0–5	1 m sbk	SiL	so ps	sh	7·5yr 3/3·5	10yr 5/3	60; 1f	Not evident
		B	5–15	1 m sbk	SiL	ss ps	sh	7·5yr 3/4	8·75yr 5/4	10; 1f	Slight fizz
		Bk	15–28	2 f sbk	SiL	ss ps	sh	7·5yr 3/4	7·5yr 4/4	70; 1f	Coats fractures
		Ck	20–40	0·5 f sbk	SiCL	s p	sh	7·5yr 4/4	7·5yr 4/4	90; 1f	Strong fizz
AD-S-1	19	A	0–4	1 f sbk	L	ss ps	sh	7·5yr 3/3	10yr 5/4	<1; 2f/m	Not evident
		B	4–29	1 m sbk	SC	ss ps	h-vh	7·5yr 3/3	10yr 5/4	<1; 1m	Not evident
		Bt	29–60	2 m sbk	C	s p	vh	7·5yr 4/4	8·75yr 5/4	<1; 1m	Not evident
		Bt2	60–135	3 m sbk	C	s p	vh-eh	7·5yr 4/4	8·75yr 5/4	<1 1m 2f	Not evident
		2Bt2	135–160	2 m sbk	C	s p	h	7·5yr 4/4	8·75yr 5/4	30; 1f	Rare coatings on basalt, < 1 mm
			Surface area: 900 m^2		Total depth: 1·8 m						
AF-R-4	94	A	0–3	1 m sbk	SL	so po	sh	7·5yr 3/3	7·5yr 5/4	45; 1f	Not evident
		B	3–10	2 m sbk	SiL	so ps	sh	7·5yr 4/4	7·5yr 5/4	10; 1f	Slight fizz
		BK	10–46	1 f sbk	SiL	ss ps	sh	7·5yr 4/4	7·5yr 5/4	75;0	Coats fractures
		Ck	46–55	1 m sbk	SiCL	ss p	sh	7·5yr 4/6	7·5yr 5/4	70;0	Along vertical fractures
AF-S-1	94	Av	0–5		L	ss ps	sh	8·75yr 4/4	10yr 5/4	<1; 1vf	Not evident
		Bt	5–20		CL	ss ps	sh-h	7·5yr 4/4	8yr 4/4	<1; 1f	Very small specs; no matrix fizz
		Bt2	20–84		SC	s p	h	7·5yr 4/4	8yr 5/4	<1; 5c 1f	Very small specs; no matrix fizz
		Btk	84–102		SC	s p	sh-h	7·5yr 4/4	8yr 5/4	<1; 2f	Filaments along roots; slight fizz on ped faces
		2Btkb	102–117		SC	s p	sh	7·5yr 4/6	8yr 5/4	40; 1f	Filaments along roots; slight fizz on ped faces
		Kb	117–170		SC	s p	h-vh	7·5yr 4/6	8yr 5/4	55–60; 1f	Stage II; abundant filaments; complete cover on pf;strong matrix fizz
		Kb2	170–195		SC	s p	sh-h	7·5yr 4/6	8yr 5/4	35; 5 vf	Stage I+; fewer visible carbs
			Surface area: 12 800 m^2		Total depth: 2·8 m						
LBM-R-1	184	A	0–3	sg	LS	so ps	lo	7·5yr 4/3	7·5yr 6/4	10	Slight fizz
		B	3–11	2 m sbk	LS	so ps	sh	7·5yr 4/4	7·5yr 6/4	<5	Under clasts
		Bk	11–26	1 f sbk	LS	so po	sh	7·5yr 4/3	7·5yr 6/4	10	Covers clasts
		K	26–48	0·5 f sbk	SL	so ps	sh	7·5yr 4/3	7·5yr 6/4	70	Stage II
LBM-S-4	184	Av	0–4	2 m p	L	ss sp	sh	8·75yr 4/3	10-yr 5/4	<1	Slight fizz
		Bw	4–10	2 m/c sbk	L	ss sp	sh	8·75yr 4/3	10-yr 5/4	<1	Sparce filaments along roots
		B	10–25	1 m sbk	LS	so po	sh	7/5yr 4/4	8·75yr 5/4	<1	Strong fizz throughout; some filaments
		Bk	25–86	1 m sbk	SL	ss so	sh	7/5yr 4/4	8·75yr 5/4	<1	Strong fizz, filaments
		Ktb	86–110	1 f/m sbk	SCL	s p	h	7/5yr 4/6	7·5yr 5/5	5–10	Small nodules; carbonates on top of clay films,1 mm coatings on clasts, carbs on ped faces
		Ktb2	110–230	2 f/m sbk	SCL	s p	h-vh	7/5yr 4/6	7·5yr 5/6	20	Thicker carbs on ped faces; abundant 2 mm + nodules,abundant carbs along roots; carbs dispersed through matrix; stage II
		Bkb	230–270	1 f sbk	SCL	s p	w-sh	7/5yr 4/6	7·5yr 5/6	20	Slight fizz, occasional specs of carbonate
		Btkb	270–290	2 f sbk	SCL	s p	sh-h	7/5yr 4/6	7·5yr 5/6	20	Slight fizz, occasional filiments and specs
		Bkb2	290–330	1 f sbk	SL	ss sp	sh	7/5yr 4/5	7·5yr 5/5	20	Very slight fizz
			Surface area*: 1125 m^2		Total depth: 3·43 m						
LBMX-R-2	263	A	0–5	1 f sbk	S	so po	so	7·5yr 4/6	7·5yr 6/4	10	Coats bottoms of clasts at surface; fizz throughout
		B	5–18	2 m sbk	S	so po	sh	7·5yr 4/5	7·5yr 6/5	<10	Fizz throughout; filiments and flakes
		K2	18–58	5 vf sbk	LS	o-ss po-p	so	7·5yr 5/4	7·5yr 5·5/4	75	Stage III; coats all clasts 2–5 mm
		K2	58–102	sg	LS	o-ss po-p	lo	7·5yr 5/3	7·5yr 7/4	75	Stage II; not as indurated as K; 1–2 mm coats on clasts
		CK	102–116	sg	LS	o-ss po-p	lo	7·5yr 6/3	7·5yr 7/3	60	Coatings on most clasts (1−<1 mm); less carbs in matrix

*Area estimated by observing extent of healthy vegetation and lack of desert pavement

Abbreviations: Structure: sg = single grain, f = fine. m = medium, c = coarse, gr = granular, sbk = subangular/blocky. Texture: S = sand, C = clay L = loam SL = sandy loam LS = loamy sand SiL = silty loam SCL = sandy clay loam SC = sandy clay SiC = silty clay. Consistency: so = non-sticky ss = slightly sticky s = sticky po = non-plastic ps = slightly plastic p = plastic sh = slightly hard h = hard vh = very hard. Roots/boundaries: vf = very fine f = fine m = medium c = coarse a = abrupt c = clear g = gradual s = smooth w = wavy i = irregular

(A)

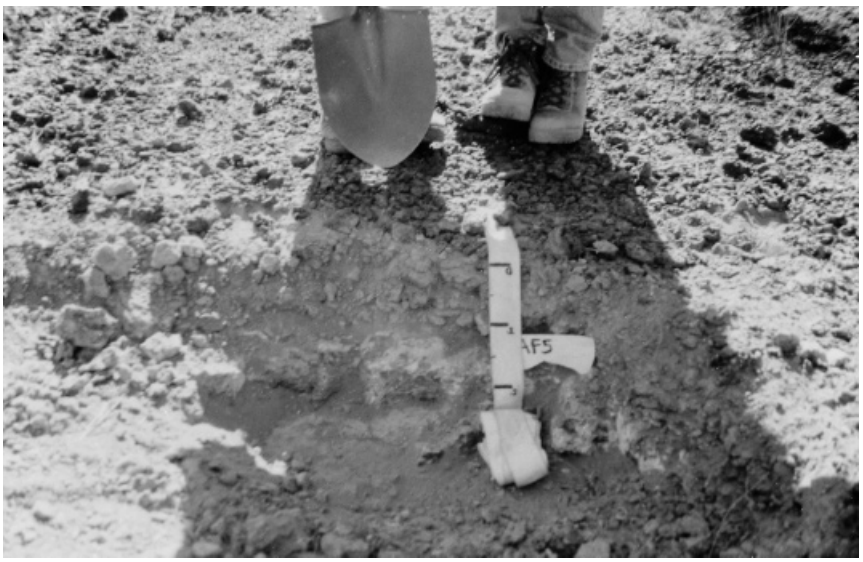

(B)

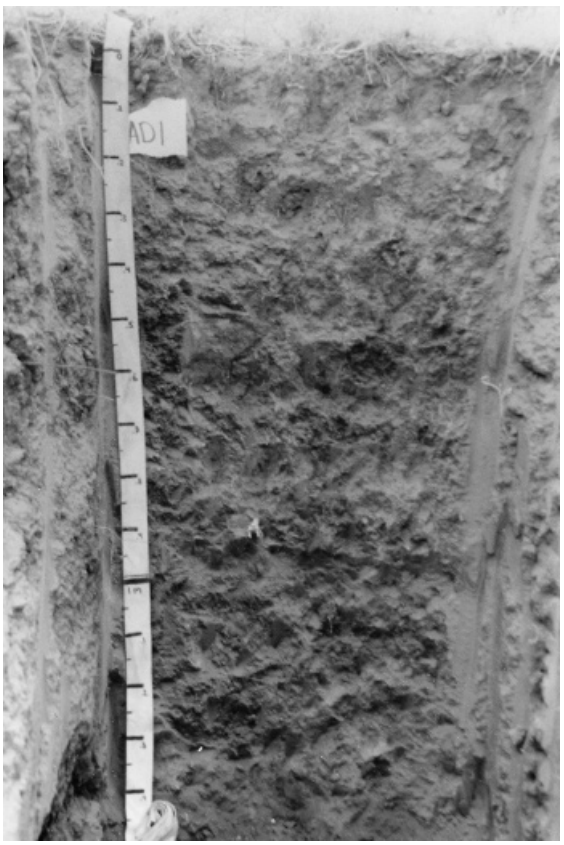

Figure 4. Photographs of typical (A) ridge and (B) swale soils

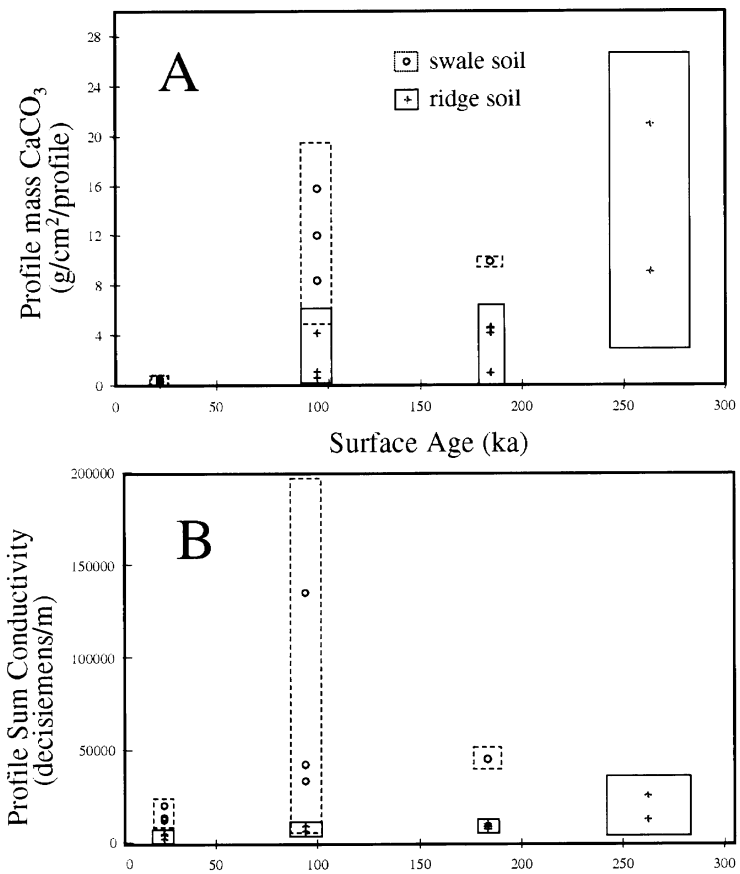

Figure 5. Graph of profile sum of (A) $CaCO_3$ and (B) electrical conductivity for ridge and swale soils of varying ages. Boxes represent analytical error for single points and standard error of the mean for multiple points

increases significantly (from 0 to 3+ mm) with the age of the surface. Ridge soil profiles contain no evidence of buried soils on any surface.

In contrast to ridge soils, swale soils are generally thick and finely textured (< 20 per cent gravel) with carbonate dispersed throughout their profiles. Clasts near the bottom of swale soil profiles have thin carbonate coatings (generally < 1 mm) which thicken slightly with age. It appears that because of thick overlying aeolian mantles, there is currently no significant loss of $CaCO_3$ through basalt fractures in swale profiles described for this study. One buried soil is present in swale pits on the *c*. 100 ka (AF) surface and two are present on the *c*. 185 ka (LBM) surface. These buried soils are characterized by sharp increases in clay and/or carbonate content below their upper Bt and K horizons. In AF-S-2, manganese coatings are present on ped faces in the uppermost buried soil.

A buried soil represents a period of relative stability in the landscape. In the cumulic environment of swale sites, a buried soil implies a period of relatively low dust flux followed by significant, rapid dust accumulation in the depression. The presence of a buried soil in swale profiles therefore implies that at least two dust flux changes have occurred during the development of the soil. The buried soil on the AF surface provides evidence for at least two changes in either (a) the regional dust flux between 20 and 100 ka, or (b) the flux of dust into swales from ridge sites at this time. The buried soils on the LBM surface suggest at least two additional changes between 100 and 180 ka.

Chemistry. Profile sum calculations of mass of carbonate and electrical conductivity suggest that, with the exception of the 20 ka AD soils, swale sites contain significantly more carbonate and salts in their soil profiles than do ridge sites (Figure 5). In arid environments, dust is a major source of $CaCO_3$ and salts for soils. Given

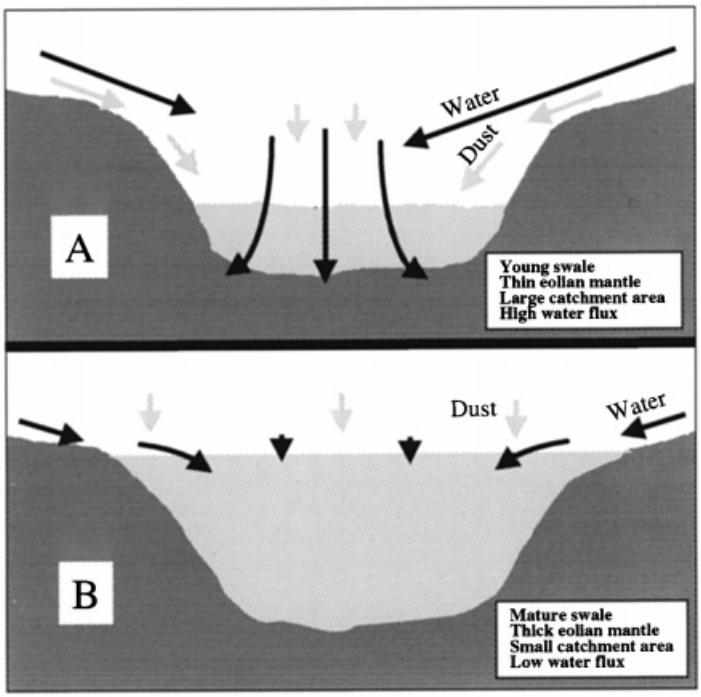

Figure 6. Schematic diagram of water and dust flux in (A) a young swale with limited dust accumulation, and (B) a mature swale with almost complete infilling. Length of arrow represents the relative amounts of water and dust entering the swale

that swale sites contain larger volumes of dust than ridge sites, this variability between ridge and swale soils was expected. Furthermore, it is likely that carbonate has been continually lost in inaccessible fractures in the underlying bedrock of ridge sites. The difference in carbonate and soluble salt content between ridge and swale soils may also be attributed to this loss. The low carbonate and salt content of both ridge and swale sites on the AD surface is possibly the combined effect of the young age of the surface and the fact that carbonate and salts are being lost along basalt fractures of both ridge and swale sites on this surface.

Stability and spatial variability. Swale soils are spatially more variable on any given basalt flow than ridge soils. This is due, in part, to the instability of these landscape positions. Swale sites are, at least initially, subject to runoff from topographic highs, and desert pavements are poorly developed. These results are similar to the Cajon Pass chronosequence, California, where soils developing in terrace swales are more variable than soils developing on bars (Harrison *et al.*, 1990). In contrast to swale soils, ridge soils are developing in relatively stable environments as evidenced by well-developed desert pavements and minimal visible effects of erosion. Morphologic and chemical spatial variability of ridge soils is low on a single basalt flow, though that variability increases slightly with age. Given the overall stability and minimal spatial variability of ridge soils, we conclude that these landscape positions would be preferable for sampling in soil chronosequence studies of the Potrillo volcanic field.

Systematic spatial and temporal variability of swale soils

Aeolian mantle accumulation and water flux. Depressions in basalt flows serve as miniature catchment basins for both dust and water. Runoff flows over basalt surfaces, entrains fine material, and washes into swales. Fine material accumulates in the swale, and runoff percolates through the aeolian mantle that has accumulated (Figure 6A), increasing the moisture conditions at the base of the swale. Similar effects of runoff on localized water availability have been documented in other arid regions (e.g. Yair and Lavee, 1985; Yair and Shachak, 1987; Yair, 1990). As the aeolian mantle of an individual swale thickens with time, catchment area and thus contribution of water from side-slopes decreases (Figure 6B). The ratio of water per volume soil

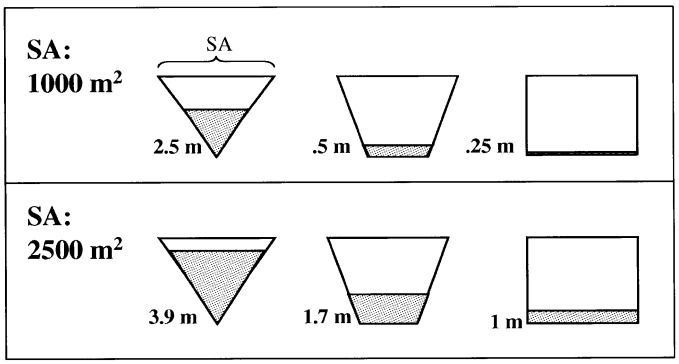

Figure 7. Calculated theoretical thickness of aeolian mantle accumulation in swales that have different surface areas (SA) and shapes. Rate of dust accumulation is assumed constant at 0·05 m^3 over a period of 50 000 years. This calculation assumes no additional accumulation via runoff from outside the swale

also decreases due to the increasing volume of dust accumulated in the swale. Consequently, a swale soil-forming environment evolves from relatively moist conditions to arid conditions through time.

The accumulation of aeolian mantle in swales is not only a function of time, but also of the size and shape of the swale being filled (Figure 7). Given equal dust flux and time, swales with similar shapes but unequal surface areas will accumulate different thicknesses of aeolian material. Swales with equal surface areas but different shapes will also accumulate dramatically different thicknesses of aeolian mantle. The size and shape of the swale will also affect the water–soil volume ratio for the depression. Simple calculations can be made for the maximum theoretical amount of precipitation/runoff from side slopes received at the aeolian mantle surface (not including evaporation/transpiration) for different shaped swales as they fill (Figure 8). Effective precipitation at the aeolian mantle surface is initially much larger than the regional mean annual precipitation for swales with significant catchment area relative to their base (i.e. cones, Figure 8). As the depression fills, effective precipitation nears regional precipitation.

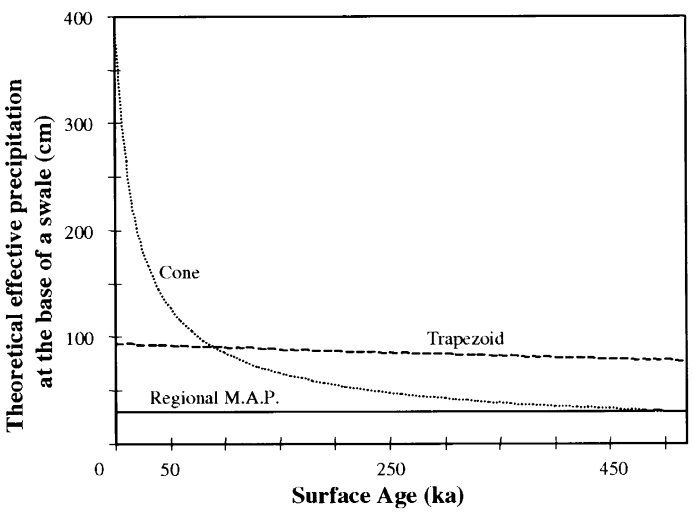

Figure 8. A graph of theoretical effective precipitation (precipitation + side-slope runoff) at the base of swales filling with aeolian material. Swales have similar surface areas but different shapes. Calculations are based on 100 per cent runoff with a constant dust accumulation rate of 0·05 $m^3 a^{-1}$. As the depression fills and area of the base of the depression approaches the surface area of the depression itself, effective precipitation approaches the mean annual precipitation (MAP) of the region. Although 100 per cent runoff is not probable, we feel that owing to the plugging of fractures with calcite on even young flows, runoff is probably high

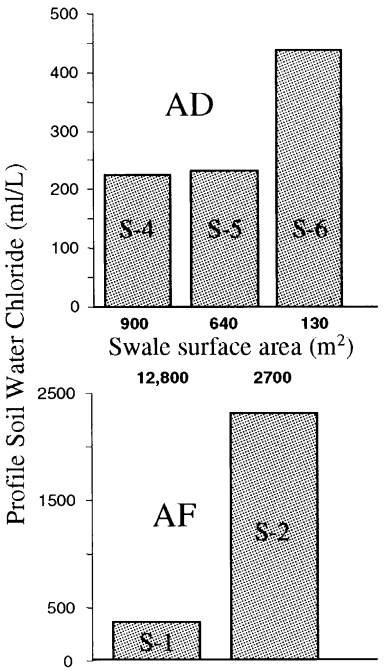

Figure 9. Graph of profile (sum of horizon concentrations) soil-water chloride concentrations for swale soils with different surface areas on the AD and AF surfaces

We find evidence for deposition-induced aridity (temporal and spatial soil variability as a function of dust accumulation) in the soil-water chloride chemistry of swale soil profiles. Owing to its extreme mobility, chloride can serve as a proxy for moisture flux in soils of arid environments (e.g. Scanlon, 1991; Murphy *et al.*, 1996). Chloride concentrations of soil water are inversely related to moisture flux in arid soils. If water flux is high enough to flush chloride through the profile, then soil-water chloride concentrations will be very low. If moisture flux is minimal, then chloride accumulates in the profile and soil-water chloride concentrations are high.

Chloride concentrations were measured for three swale soils on the AD surface, and two swale soils on the AF surface (Figure 9). The AD-S-6 and AF-S-2 soils have significantly higher profile chloride concentrations than the other swale soils on those surfaces. These chloride concentrations suggest that the current moisture fluxes of the AD-S-6 and AF-S-2 soils are relatively low. Both of these swales are the smallest-sized depressions described for each surface and are already in a mature phase (Figure 6 B) of aeolian accumulation compared to other swales sampled. We suggest that the low water flux in the AD-S-6 and AF-S-2 swale soils is a result of the relatively complete infilling of these depressions. Furthermore, we find evidence that the current state of aridity in the AF-S-2 soil has not been constant. The depth profile of chloride concentrations for the AF-S-2 soil contains a bulge followed by a sharp decrease with depth (Figure 10). This common feature of desert soils often signifies higher past water fluxes in the profile (Scanlon, 1991; Phillips, 1994). Also, manganese coatings on ped faces provide further evidence for higher moisture conditions in the past (Weitkamp *et al.*, 1996) for the AF-S-2 buried soil. Since these features are not observed in other soils, we suggest that the changing environmental conditions that have affected the AF-S-2 soil result from in-filling of the swale in which it is forming.

Evidence for variable rates of infilling of different-sized/shaped swales is found on the AF surface. Buried soils in a cumulic soil environment (swales) represent a hiatus in regional dust deposition and can therefore act as a temporal marker in the entire landscape. A buried soil will thus represent the varying heights of the aeolian mantle in different swales at the time that regional dust deposition was low. A buried soil is found in swale soils of the AF surface. The buried soil in AF-S-2, a small (*c.* 3000 m^2), relatively narrow depression, is

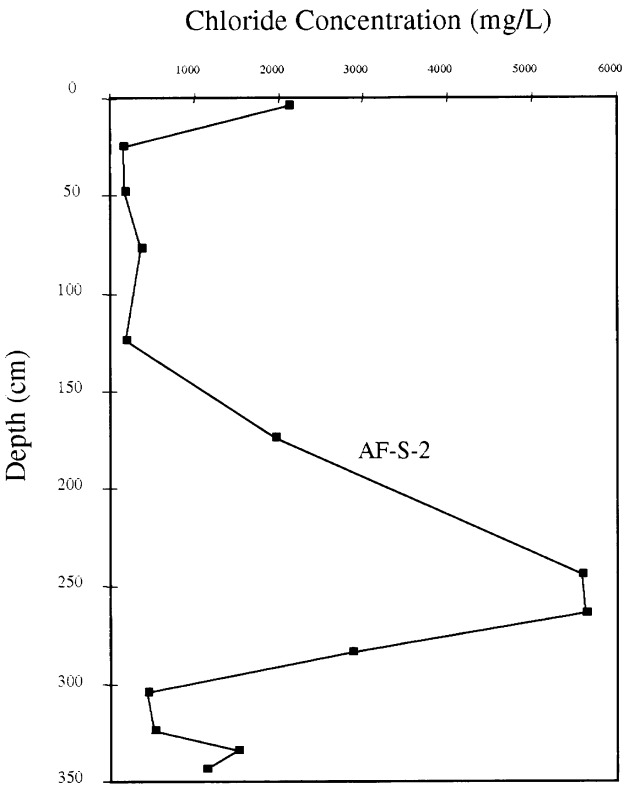

Figure 10. Depth profile of soil water chloride concentrations in the AF-S-2 soil

found at a depth of approximately 1 m. The buried soil in the large (*c.* 13 000 m^2) AF-S-1 profile is located in the rubble zone at a depth of approximately 2 m. This difference in the location of the buried soil in AF-S-1 and AF-S-2 suggests that AF-S-1 had a significantly thinner aeolian mantle than AF-S-2 at the time when the buried soils developed. Furthermore, the small AF-S-2 swale currently contains 3·5 m of aeolian mantle, compared to <2 m in the large AF-S-1 swale, reaffirming the effects of size and shape on infilling rates of depressions.

Surface stability. Variation in the rate of accumulation of aeolian material in swales should not only affect the hydrologic characteristics of the soil-forming environment, but also the stability. While a swale is filling with aeolian material, the soil in that depression will be cumulic. When a depression is completely filled, however, the rate of dust accumulation is significantly reduced. Consequently, the surface becomes relatively stable. Therefore, for any one isochronous basalt flow, there should be a number of geomorphic surfaces of varying age and with varying degrees of soil development (Figure 11). We see evidence for this systematic spatial variability on the AF surface. The AF-S-3 swale is small (<30 m^2), with minimal relief. It is considerably smaller than AF-S-2 (*c.* 3000 m^2). Given the stability model suggested above, we would expect greater soil development in this profile. The surface of the AF-S-3 depression has a better developed desert pavement than that of AF-S-1 and AF-S-2, and has reached stage III carbonate development, while AF-S-1 and AF-S-2 both display stage II carbonate development. These changes from time-transgressive soils to stable soils further add to the complexity of the variability of swale soils on basalt flows in the Potrillo volcanic field. The fact that ridge sites have remained stable since emplacement of the basalts further supports them as the landscape position from which to sample soils in a future chronosequence study.

Implications for aquifer recharge. The high moisture flux conditions observed in swale soils of the Potrillo volcanic field have implications for local aquifer recharge. There are two schools of thought concerning

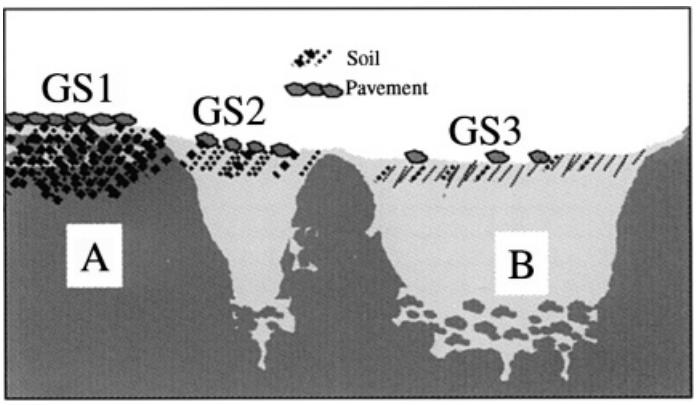

Figure 11. Schematic representation of three geomorphic surfaces (GS1, GS2, GS3) on an isochronous basalt flow. The degree of soil and desert pavement development (represented by concentration of lines and pebbles) is a function of the timing of the stability of the surface. That timing is in turn a function of the size and shape of the swale in which aeolian material is accumulating. (A) Ridges become stable essentially at the time of basalt deposition and have well developed soils. (B) Large broad swales are the last to become stable and have poorly developed soils

aquifer recharge from desert vadose zones. One suggests that desert soils are stable environments characterized by minimal water and solute flux as evidenced by bulges in soil-water chloride concentrations close to the land surface (Phillips, 1994). However, a drop in chloride concentrations below this bulge has been widely documented in desert soils. In keeping with the idea of a hydrologically stable vadose zone, the generally accepted interpretation for this drop is that it is a result of palaeoclimatic variations (Scanlon, 1991). Some studies have shown, however, that preferential flow of water through desert vadose zones is common (e.g. Yair and Shachak, 1987), and it is suggested that changes with depth in soil-water chloride concentrations could be a result of surficial short-term temporal and spatial variability (Hendrickx and Dekker, 1991; Spijkers, 1994). The short-term time scale implication of a changing moisture flux with changing surface conditions is that desert vadose zones are potentially significant contributors to local aquifer recharge. Data from the Potrillo volcanic field support this latter theory. Moisture fluxes are high in depressions that are still receiving large amounts of runoff and have not yet filled with aeolian material.

Furthermore, average maximum chloride concentrations for swale soils in the Potrillos (excluding Av horizons) fall around 300 mg l^{-1} (Table III). Maximum concentrations reported by Scanlon (1991) for an area just south of the Potrillos are between 2000 and 3000 mg l^{-1}. Phillips (1994) reports averages around 3000 mg l^{-1} for a similar area. The difference in these data suggests that water flux through soils developing in depressions on basalt flows is significantly larger than that of other soils in the region. Given that basalt flows in the Potrillo volcanic field occupy over 200 km^2, these larger moisture fluxes could provide significant aquifer recharge through a single basalt flow. Considering that >10 per cent of the land area of New Mexico is covered with basalts, it is possible that recharge through these surfaces could play an important role in aquifer recharge for the entire state.

CONCLUSIONS

Systematic spatial variability of soils in the Potrillo volcanic field is primarily a function of whether soils are developing on ridges or swales of basalt flow topography. The systematic spatial and temporal variability of swale soils is complex, while observable systematic spatial variability of ridge soils is minimal. We therefore conclude that ridge soils should be used as the primary basis for chronosequence studies in this area. The systematic variability of swale soils has implications for chronosequence studies as well as for soil and palaeoclimate studies. Observed high water flux through large swales suggests that these sites may be areas of aquifer recharge. Ridge soils do not provide evidence for this potential aquifer recharge nor for the changes in

Table III. Soil-water chloride values for three typical swale soils

Soil	Age (ka)	Horizon	Depth (cm)	Soil-water chloride ($g\ ml^{-1}$)
AD-S-1	20	A	0–4	2634·6
		B	4–29	290·0
		Bt	29–60	128·0
		Bt2	60–80	271·0
			80–100	232·3
			100–120	104·5
			120–135	118·2
		2Bt2	135–150	73·1
			150–170	92·3
			170–190	83·2
AF-S-1	100	Av	0–5	1836·7
		Bt	5–20	1170·5
		Bt2	20–40	473·1
			40–60	103·5
			60–84	273·9
		Btkb	84–102	191·2
		2Btkb	102–117	55·8
		Kb	117–137	104·2
			137–157	92·5
			157–170	119·9
		Kb2	170–195	110·7
		Ck	195–220	67·8
			220–240	134·9
			240–260	94·3
LBM-S-4	185	Av	0–4	8435·7
		Bw	4–10	388·4
		B	10–25	388·4
		Bk	25–86	184·7
		Ktb	86–110	163·9
		Ktb2	110–130	218·6
			130–150	123·8
			150–170	217·2
			170–190	144·3
			190–210	144·3
			210–230	224·5
		Bkb	230–250	741·3
			250–270	234·8
		Btkb	270–290	169·0
		Bkb2	290–310	134·2
		C	310–330	241·2
			330–350	274·8
			350–370	353·3

regional dust flux that were also observed in swale soils. Although soil chronosequence development was the primary objective for this spatial variability study, only by investigating the entire spectrum of soils available in the study area could these important environmental conditions of the Potrillo volcanic field have been recognized.

REFERENCES

Anthony, L. and Poths, J. 1992. '^{3}He surface dating and its implications for magma evolution in the Potrillo volcanic field, Rio Grande Rift, New Mexico, USA,' *Geochimica et Cosmochimica*, **56**, 4105–4108.

Barrett, L. and Schaetzl, R. 1993. 'Soil development and spatial variability on geomorphic surfaces of different age,' *Physical Geography*, **14**, 39–55.

Bockheim, J. 1980. 'Solution and use of chronofunctions in studying soil development,' *Geoderma*, **24**, 71–85.

Cerling, T. 1990. 'Dating geomorphologic surfaces using cosmogenic ^{3}He,' *Quaternary Research*, **33**, 148–156.

Gile, L., Hawley, L. and Grossman, R. 1981. Soils and Geomorphology in the Basin and Range Area of Southern New Mexico, Guidebook to the Desert Project, New Mexico Bureau of Mines and Mineral Resources, Memoir **39**.

Harrison, J. and Yaalon, D. 1992. 'Soils developed on late Pleistocene till, Medicine Bow Mountains, Wyoming (Discussion and

Reply),' *Soil Science*, **154**(3), 250–254.
Harrison, J., McFadden, L. and Weldon, R. 1990. 'Spatial soil variability in the Cajon Pass chronosequence: Implications for the use of soils as a geochronological tool,' *Geomorphology*, **3**, 399–416.
Hendrickx, J. and Dekker, L. 1991. 'Experimental evidence of unstable wetting fronts in non-layered soils,' in Proceedings of the National Symposium on Preferential Flow, American Society of Agricultural Engineers, 22–31.
Hoffer, J. 1976. Geology of Potrillo basalt field, south central New Mexico, New Mexico Bureau of Mines and Mineral Resources, Circular 149.
Jenny, H. 1941. Factors of Soils Formation, McGraw-Hill, New York, 281 pp.
Machette, M. 1985. 'Calcic soils of the southwestern United States,' in Weide, D. (Ed.), Soils and Quaternary Geomorphology of the Southwestern United States, Geological Society of America, Special Paper 203, 1–21.
McDonald, E. 1994. The relative influences of climatic change, desert dust, and lithologic control on soil-geomorphic processes and hydrology of calcic soils formed on Quaternary alluvial-fan deposits in the Mojave Desert, California, PhD dissertation, University of New Mexico, 383 pp.
McDougall, I. and Harrison, M. 1988. Geochronology and Thermochronology by the ^{40} Ar/^{39} Ar Method, Oxford University Press, New York.
Murphy, E., Ginn, T. and Phillips, J. 1996. 'Geochemical estimates of paleorecharge in the Pasco Basin: Evaluation of the chloride mass balance technique,' *Water Resources Rresearch*, **32**(9), 2853–2868.
Phillips, F. 1994. 'Environmental tracers for water movement in desert soils of the American Southwest,' *Soil Science Society of America Journal*, **58**(1), 15–24.
Scanlon, B. 1991. 'Evaluation of moisture flux from chloride data in desert soils,' *Journal of Hydrology*, **28**, 137–156.
Schaetzl, R., Barrett, L. and Winkler, J. 1994. 'Choosing models for soil chronosequences and fitting them to data,' *European Journal of Soil Science*, **49**(2), 219–232.
Singer, M. and Janitzky, P. (Eds) 1986. Field and laboratory procedures used in a soil chronosequence study, Bulletin 1648, US Geological Survey, Denver, Colo.
Slate, J., Bull, W., Ku, T., Shafiqullah, M., Lynch, D. and Huang, Y. 1991. 'Soil-carbonate genesis in the Pinacate volcanic field, northwestern Sonora, Mexico,' *Quaternary Research*, **35**, 400–416.
Soil Survey Staff 1951. Soil Survey Manual, Agricultural Handbook 18, US Department of Agriculture and US Government Printing Office, Washington, DC.
Soil Survey Staff 1975. Soil Taxonomy, Agriculture Handbook 436, US Department of Agriculture and US Government Printing Office, Washington, DC.
Sondheim, M. and Standish, J. 1983. 'Numerical analysis of a chronosequence including an assessment of variability,' *Canadian Journal of Soil Science*, **63**, 501–517.
Spijkers, T. 1994. In situ field experiments to determine the soil physical characteristics of soils under conventional and not-tillage management systems, MS thesis, Hydrology program, New Mexico Tech., Socorro, NM.
Switzer, P., Harden, J. and Mark, R. 1988. 'A statistical method for estimating rates of soil development and ages of geological deposits: A design for soil chronological studies,' *Mathematical Geology*, **20**, 49–61.
United States Weather Bureau 1996 Climatological summary for Las Cruces, New Mexico, US Department of Commerce, Albuquerque.
Weitkamp, W., Graham, R., Anderson, M. and Amrhein, C. 1996. 'Pedogenesis of a Vernal Pool Entisol-Afisol-Vertisol Catena in Southern California,' *Soil Science Society of America Journal*, **60**(1), 323 pp.
Wells, S., Dohrenwned, J., McFadden, L., Turrin, B. and Mahrer, K. 1985. 'Late Cenozoic landscape evolution on lava flow surfaces of the Cima volcanic field, Mojave Desert, California,' *Geological Society of America Bulletin*, **96**, 1518–1529.
Wilding, L. and Drees, L. 1983. 'Spatial variability and pedology,' in Wilding, L. (Ed) Pedogenesis and Soil Taxonomy, Elsevier Science, Amsterdam, 83–116.
Yair, A. 1987. 'Environmental effects of loess penetration into the Negev Desert,' *Journal of Arid Environments*, **13**, 8–24.
Yair, A. 1990. 'Runoff generation in a sandy area - The Nizzana sands, western Negev, Israel,' *Earth Surface Processes and Landforms*, **15**, 597–609.
Yair, A. and Lavee, H. 1985. 'Runoff generation in arid and semi-arid zones,' in Anderson, M. and Burt, T. (Eds), Hydrological Forecasting, Wiley and Sons, New York, 183–220.
Yair, A. and Shachak, M. 1987. 'Studies in watershed ecology of an arid area,' in Berkofsky, L. and Wurtele, M. (Eds), Progress in Desert Research, Rowman and Littlefield, Totowa, N.J., 145–193.

